Non-destructive assessment of rebar corrosion based on equivalent structural parameters using peizo-transducers

V. Talakokula[1], S. Bhalla[2,*], B. Bhattacharjee[2] and A. Gupta[2]

[1]Department of Civil Engineering, ABES Engineering College, Ghaziabad 201 009, India
[2]Department of Civil Engineering, Indian Institute of Technology Delhi, Hauz Khas, New Delhi 110 016, India

Occurrence of corrosion in rebars of reinforced concrete (RC) structures is a common problem faced by the ageing infrastructure across the world. This article presents a newly developed approach for detecting and quantifying corrosion of steel bars utilizing a piezoelectric ceramic (PZT) patch surface-bonded on the rebars employing equivalent structural parameters using the electro-mechanical impedance (EMI) technique. This technique utilizes the electro-mechanical coupling property of piezoelectric materials for a damage diagnosis. Through tests on three steel rebars, empherical relations are derived to relate the corrosion-induced mass and stiffness loss to the loss in the equivalent mass and stiffness identified by the PZT patch. The equivalent mass loss and stiffness loss correlate well with the actual mass loss and stiffness loss and, provide an alternative corrosion assessment paradigm suitable for diagnosing corrosion in steel rebars. The model-based corrosion assessment presented can be utilized for real-life steel structures.

Keywords: Electro-mechanical impedance technique, piezoelectric ceramic sensors, reinforced concrete, steel.

CORROSION is defined as the undesirable deterioration of a metal or an alloy caused by its interaction with the environment that adversely affects the properties of the metal/alloy, which should otherwise be preserved. Interest of the scientific community in corrosion has been increasing because of the wastage of precious metal, apart from endangering the structural performance and inducing failure. The present study deals with the corrosion in steel rebars, which has been identified as the most common cause of deterioration and premature failure of reinforced concrete (RC) structures[1]. Reinforcement corrosion induced structural failure does not necessarily imply structural collapse, but in most cases manifests as the loss of structural serviceability, characterized by concrete spalling and the excessive deflection of the affected RC members[2]. Practical experience and experimental observations suggest that corrosion-affected RC structures deteriorate at different rates as measured by strength and serviceability, with the latter deteriorating at a much faster rate. The reason for this is attributed to the fact that the corrosion products exert an expansive pressure on the concrete. Due to the low tensile strength of concrete, this expansive pressure leads to concrete cracking, spalling and debonding between the reinforcement and the surrounding concrete; all these effects soon become prominent once corrosion actively propagates in the structure. As a consequence, the stiffness of the structure reduces and deflection increases[3,4].

This article extends the application of a new approach developed for assessment of corrosion in steel rebars. While our previous studies were on the corrosion assessment in RC structures and comparison of sensing abilities of the surface bonded with that of embedded sensor for corrosion assessment in RC structures, the present article focuses on bare steel bars using surface-bonded sensors. The results obtained can be a basis for assessing the corrosion in real-life steel structures. The article first presents a brief description of the electro-mechanical impedance (EMI) technique, followed by details of the specific experiments conducted on steel rebar specimens and the development of empirical equivalent models based on the measured electromechanical data.

Electro-mechanical impedance technique

The piezoelectric ceramic (PZT) patch has a unique property of generating surface charges on application of mechanical stress known as direct effect. Conversely it undergoes mechanical deformation when subjected to electric fields. These direct and the converse effects are illustrated in Figure 1.

The EMI technique using PZT patches is a relatively new technique for structural health monitoring (SHM). The technique was invented by Liang *et al.*[5] and further developed by several research groups[6–13]. The EMI technique has been experimentally found to be powerful in detecting localized incipient damage in a variety of structures[14–20]. In this technique, a PZT patch is surface-bonded to the monitored structure as shown in Figure 2 and electrically excited by means of an impedance analyser/LCR meter. Under external field excitation, the bonded

*For correspondence. (e-mail: sbhalla@civil.iitd.ac.in)

patch induces deformations in the host structure, whose response is transferred back to the patch in the form of admittance function, consisting of conductance and susceptance. This admittance signature acquired over a high frequency range (30–400 kHz), forms the benchmark for assessing the structural health. At any future point of time, when it is desired to assess the health of the structure, the signature is acquired again and compared to the baseline signature, any deviation of which provides an indication of damage.

The electrical admittance of the piezo-transducer can be expressed as a function of the mechanical impedance of the transducer and the drive point mechanical impedance of the host structure by means of a coupled equation derived by Liang *et al.*[5], who first proposed the impedance approach to model PZT–structure electro-mechanical interaction in 1D structures. Bhalla *et al.*[15] extended the impedance formulations to 2D by introducing the concept of 'effective impedance' and derived a modified expression for the complex electro-mechanical admittance $\bar{Y}$ *as*

$$\bar{Y} = \frac{\bar{I}}{V} = G + Bj = 4\omega j \frac{l^2}{h}\left[\overline{\varepsilon_{33}^T} - \frac{2d_{31}^2 \overline{Y^E}}{(1-\nu)} + \frac{2d_{31}^2 \overline{Y^E}}{(1-\nu)} \times \left(\frac{Z_{a,\text{eff}}}{Z_{s,\text{eff}} + Z_{a,\text{eff}}}\right)\left(\frac{\tan kl}{kl}\right)\right], \quad (1)$$

where h is the thickness of the patch, ν the Poisson's ratio, $Z_{a,\text{eff}}$, the short-circuited effective mechanical impedance of the PZT patch, $Z_{s,\text{eff}}$, the mechanical impedance of the host structure and ω the angular frequency. Mechanical impedance of the host structure depends on its mass, stiffness and damping properties. Damage in the structure alters these structural properties and hence the mechanical impedance, which is reflected in the electrical admittance of the piezo-transducer.

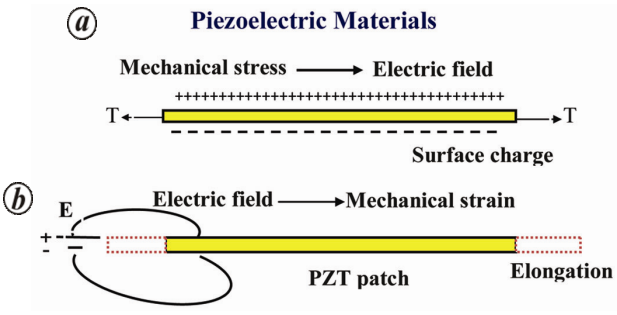

Figure 1. (*a*) Direct (sensor) and (*b*) converse (actuator) effects of piezoelectric materials.

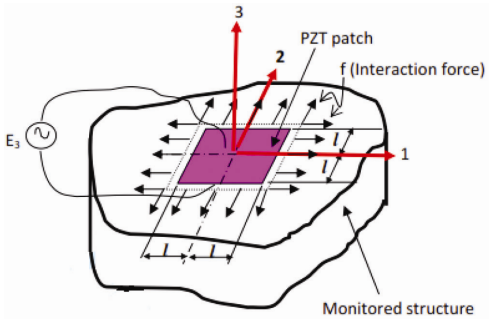

Figure 2. Modelling PZT–structure interaction using effective impedance approach[6].

The subsequent sections cover a description of the rebar experimental specimens, their testing under accelerated corrosion in the laboratory, monitoring the process using the EMI technique, extracting equivalent parameters from the admittance signature and developing an equivalent mass model based on measured data.

Assessment of corrosion in steel rebars using electro-mechanical impedance technique

Corrosion is monitored basically using electrochemical techniques; a detailed review of the corrosion monitoring techniques along with their applications is given by Rothwell[21]. The most commonly used electrochemical technique for corrosion assessment is the open circuit potential measurement (half-cell potential) technique. The half-cell potential, which is the measure of the electrode potential, equals the potential difference between steel and the adjacent concrete electrolyte, and hence is a property of steel/concrete interface. Thus, in a given concrete environment, it may serve as an indicator of rebar corrosion initiation since the threshold of depassivation depends mainly on the electrode potential compared to other factors[22]. This technique detects the likelihood of corrosion of steel at a given location and time, but cannot indicate the rate of corrosion[23]. While interpreting the half-cell potential data, one must also consider factors such as oxygen and chloride concentrations and concrete electrical resistance, all of which have a significant influence on the readings[24]. Hence there is a need of a sensing technique which can remotely operate and assess the condition of the structure. It is now recognized that in the total management of structures, which involves both whole-life economics and life cycle estimations, integrated monitoring systems and procedures have an important role. For this purpose, effective corrosion sensor technology is critical for ensuring safety of RC structures during their lifetime.

The newest generation of autonomous SHM systems with active sensors can possibly extract more information of the current and future performance of the structure. Extensive analytical and experimental works have been devoted to the detection of corrosion in concrete structures using fibre optic sensors[25–30]. However, only limited studies have been reported for corrosion detection using PZT patches. Proof of concept experiments to detect corrosion using PZT patch in metallic structures have been reported[31–34]. Our previous studies presented the corrosion

assessment in RC structures using surface bonded as well as embedded sensors[35,36], confining the rebar with surrounding concrete. The present study is aimed at developing dimensionless parameters when the piezo sensor surface bonded to the rebar is unconfined.

Experimental details

Three high yield deformed (HYD) steel rebars of 300 mm length and 16 mm diameter were surface-bonded with square PZT patches of size 10 × 10 × 0.3 mm and grade PIC151 (ref. 37). All the rebars were machined in the central portion so as to achieve a smooth surface to bond the patch (Figure 3 *a*). A thin layer of two part Araldite epoxy adhesive was applied on the machined surface and the PZT patch was placed on it. Light pressure was applied over the assembly using small weight. The set-up was left undisturbed in this condition at room temperature for 24 h to enable full curing of the adhesive. The electrodes were then soldered to the PZT patch and attached to Agilent E4980A LCR meter[38] (Figure 3 *b*). In this manner, the electro-mechanical admittance signature, consisting of the real part (conductance *G*) and the imaginary part (susceptance *B*) was acquired in a frequency range 100–300 kHz for all the three rebars. A frequency interval of 100 Hz was used for each admittance measurement. All the tests were performed under controlled laboratory conditions so that the temperature fluctuations could be ruled out.

Under normal environmental conditions, corrosion of a rebar is a relatively slow process, often taking several years to progress significantly. In order to obtain data in a reasonable time-frame for a laboratory-based study, the corrosion was accelerated using impressed current using anodic method[27–30]. After the baseline admittance signatures were acquired, the specimens were placed in a beaker containing 'brine' solution (of salinity 35 parts per thousand). An electrical loop was set up with the steel rebar specimens forming the anode and the negative terminal was connected to a copper bar dipped in the solution acting as cathode (Figure 4). To accelerate the corrosion process, a constant current of 150 μA/cm^2 was applied to the specimen using fixed power supply device (model ST 4076)[39] for a period of 8 h. The admittance signatures were acquired for each specimen at regular intervals after each hour of accelerated corrosion exposure. Before any signature acquisition, the rebars were taken out of the brine solution, wiped clean of water and dried under a fan. It was ensured that the PZT patch was always above the top layer of the brine solution, i.e. the PZT patch was never submerged in the solution (as shown in Figure 4).

Figure 5 shows the condition of one the rebars before and after exposure to accelerated corrosion. As clearly visible from the figure, substantial corrosion has occurred in the bar after 8 h of application of constant current, whereas when the same rebar is embedded in concrete it took 120 days for substantial corrosion to occur[35,36]. From this, it can be concluded that the bare rebars are more susceptible to corrosion and hence before embedding them in concrete it must be ensured that the corrosion is not severe. The distance of the affected region (corroded area as shown in Figure 5 *b*) from the PZT patch is within its zone of influence of the patch, which typically extends to about 1 m in such 1D structures[9]. The conductance signatures obtained from the sensor are shown in Figure 6.

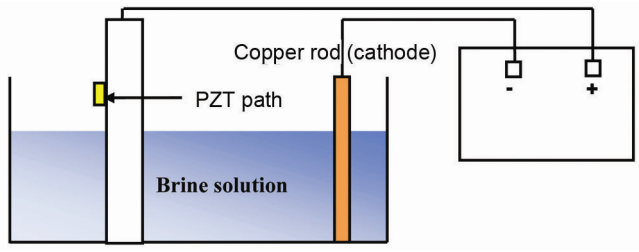

Figure 4. Accelerating corrosion set-up.

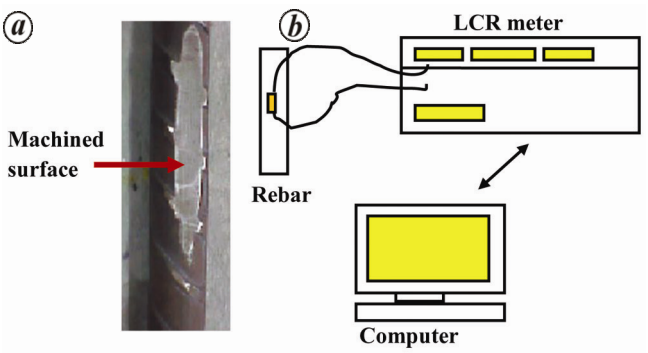

Figure 3. Data acquisition set-up. ***a***, Rebar specimen prepared for bonding PZT; ***b***, Experimental set-up.

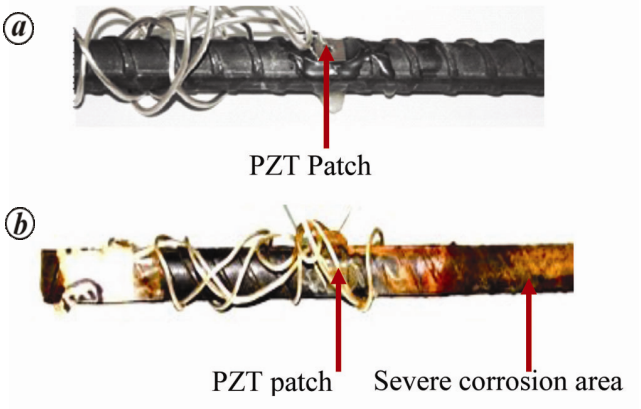

Figure 5. Condition of specimens: ***a***, Pristine specimen; ***b***, Corroded specimen.

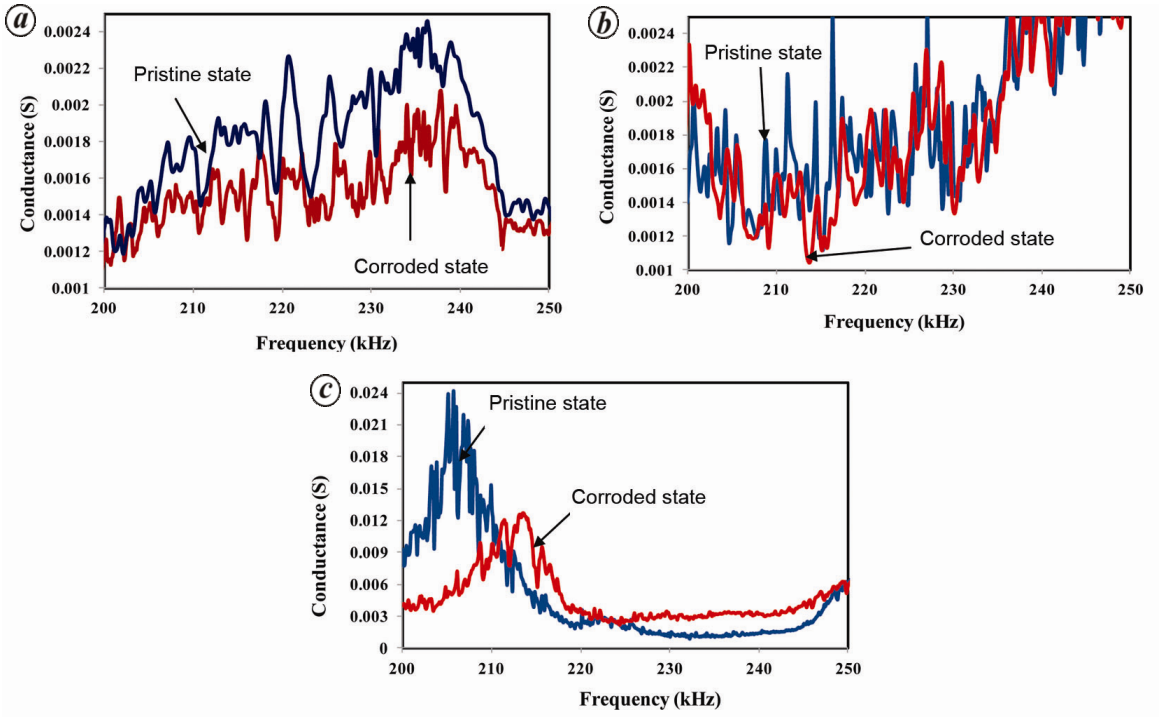

Figure 6. Variation of conductance signature due to accelerated corrosion exposure: ***a***, Specimen 1; ***b***, Specimen 2; ***c***, Specimen 3.

The variation of G (real part of admittance) of the PZT patches bonded to the rebar specimens is considerable and the signature can be observed to change substantially with corrosion for all the three specimens as shown in figures. The conductance signatures vary from specimen to specimen, as they depend on a number of factors such as bonding conditions of the patch, local surface and variability of the PZT parameters. Further, the overall effect of exposure may have small variation from specimen to specimen. From the marked difference in the signature of corroded state from the pristine state of each specimen, it can be concluded that the mechanical impedance has changed due to corrosion. This happens because the corrosion changes the mass, stiffness and/or damping properties of the bar, which in turn causes the conductance signature to change in accordance with eq. (1).

Authors have earlier proposed a method for assessment of corrosion using the equivalent structural parameters extracted from impedance spectrum. The present study extends the application of this method to bare steel rebars. The next section compares the advantages of the proposed method with the existing method of damage quantification and conventional method of corrosion detection.

Identification of equivalent system

The electro-mechanical admittance (given by eq. (1)) can be decomposed into active and passive parts as

$$\underbrace{\bar{Y} = 4\omega j \frac{l^2}{h}\left[\overline{\varepsilon_{33}^T} - \frac{2d_{31}^2 \overline{Y^E}}{(1-\nu)}\right]}_{\text{Passive part}} + \underbrace{\frac{8\omega d_{31}^2 \overline{Y^E} l^2}{(1-\nu)}\left(\frac{Z_{a,\text{eff}}}{Z_{s,\text{eff}} + Z_{a,\text{eff}}}\right)\bar{T}j}_{\text{Active part}}, \quad (2)$$

or

$$Y = Y_{\text{P}} + Y_{\text{A}}. \quad (3)$$

Using the computational procedure outlined by Bhalla *et al.*[40], the real and imaginary components (x and y respectively) of the structural impedance i.e. $Z_{s,\text{eff}}$ can be determined as

$$Z_{s,\text{eff}} = x + yj, \quad (4)$$

where

$$x = \frac{M(x_a R - y_a S) + N(x_a S + y_a R)}{M^2 + N^2} - x_a, \quad (5)$$

$$y = \frac{M(x_a R + y_a S) - N(x_a S - y_a R)}{M^2 + N^2} - y_a, \quad (6)$$

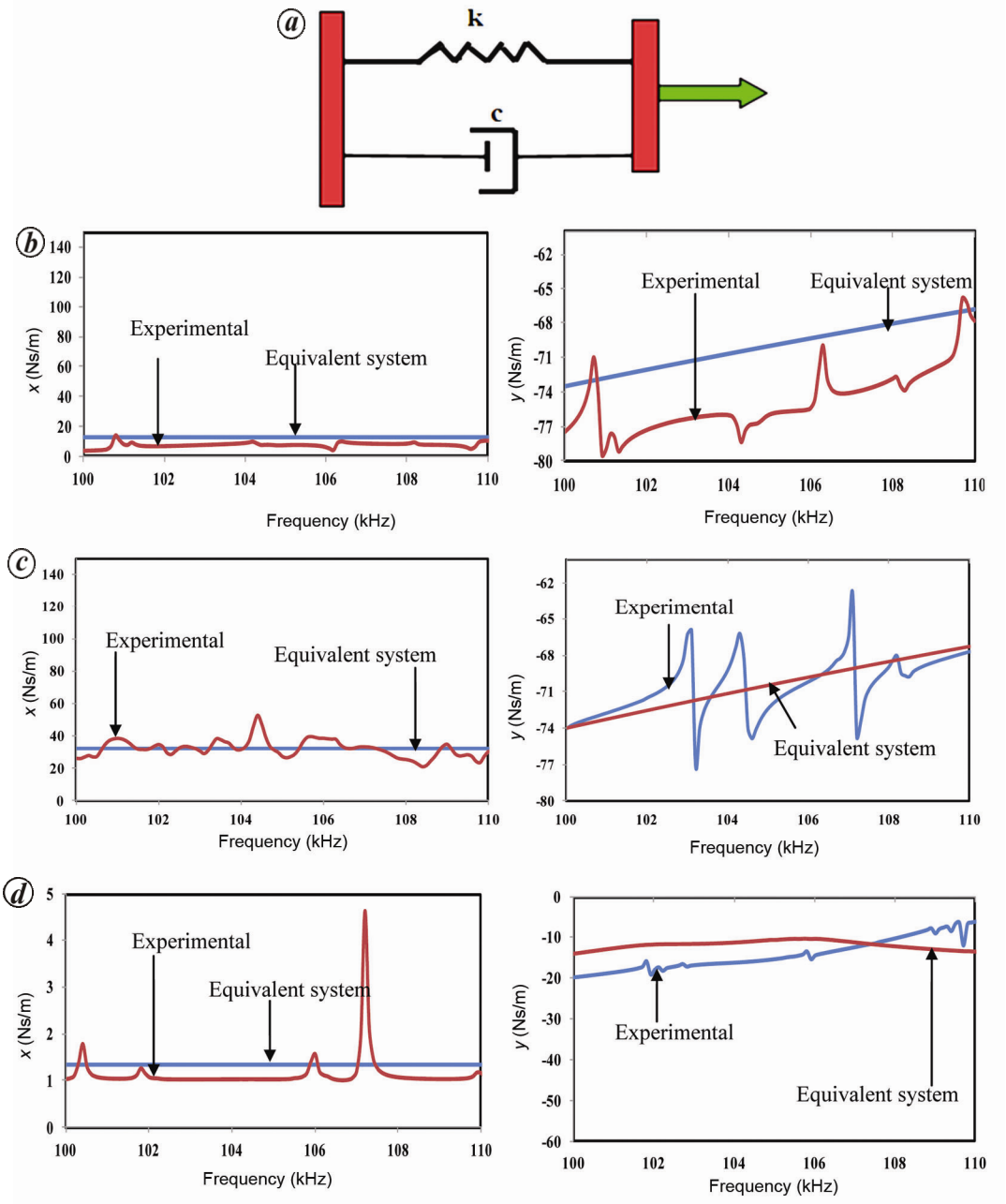

Figure 7. ***a***, Equivalent system. ***b–d***, Comparison of experimental plots x and y with those of identified system for: ***b***, Specimen 1; ***c***, Specimen 2; ***d***, Specimen 3.

$$M = \frac{B_A h}{4\omega K l^2} \text{ and } N = -\frac{G_A h}{4\omega K l^2}, \tag{7}$$

and

$$R = r - \eta t,\ S = t + \eta r,\ K = \frac{2d_{31}^2 \overline{Y^E}}{(1-\nu)}. \tag{8}$$

G_A and B_A are the real and the imaginary components of the active admittance, computed from

$$\overline{Y}_A = \overline{Y} - \overline{Y}_P, \tag{9}$$

and $Z_{a,\text{eff}} = x_a + y_a j$ is the effective mechanical impedance of the PZT patch. Depending upon the variation of x and y with frequency and the associated values, the inherent elements (stiffness k, mass m and damping c) making the host structural system can be identified by Hixon[41], as shown in Figure 7 *a*.

The experimental signature of the PZT patches bonded to the three specimens consists of G and B over 100–300 kHz range. Using eqs (1), (5) and (6), the mechanical impedance of the host structure (here steel rebars) was obtained at each frequency using the already established computational procedure[40]. The extracted mechanical

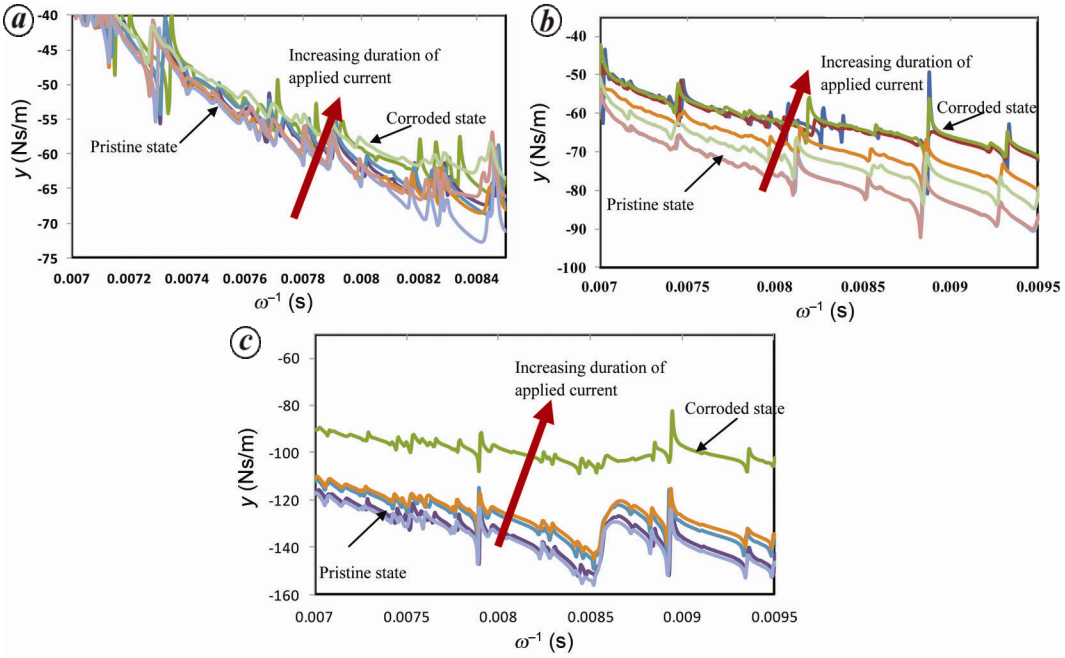

Figure 8. Variation of y with ω^{-1}. ***a***, Specimen 1; ***b***, Specimen 2; ***c***, Specimen 3.

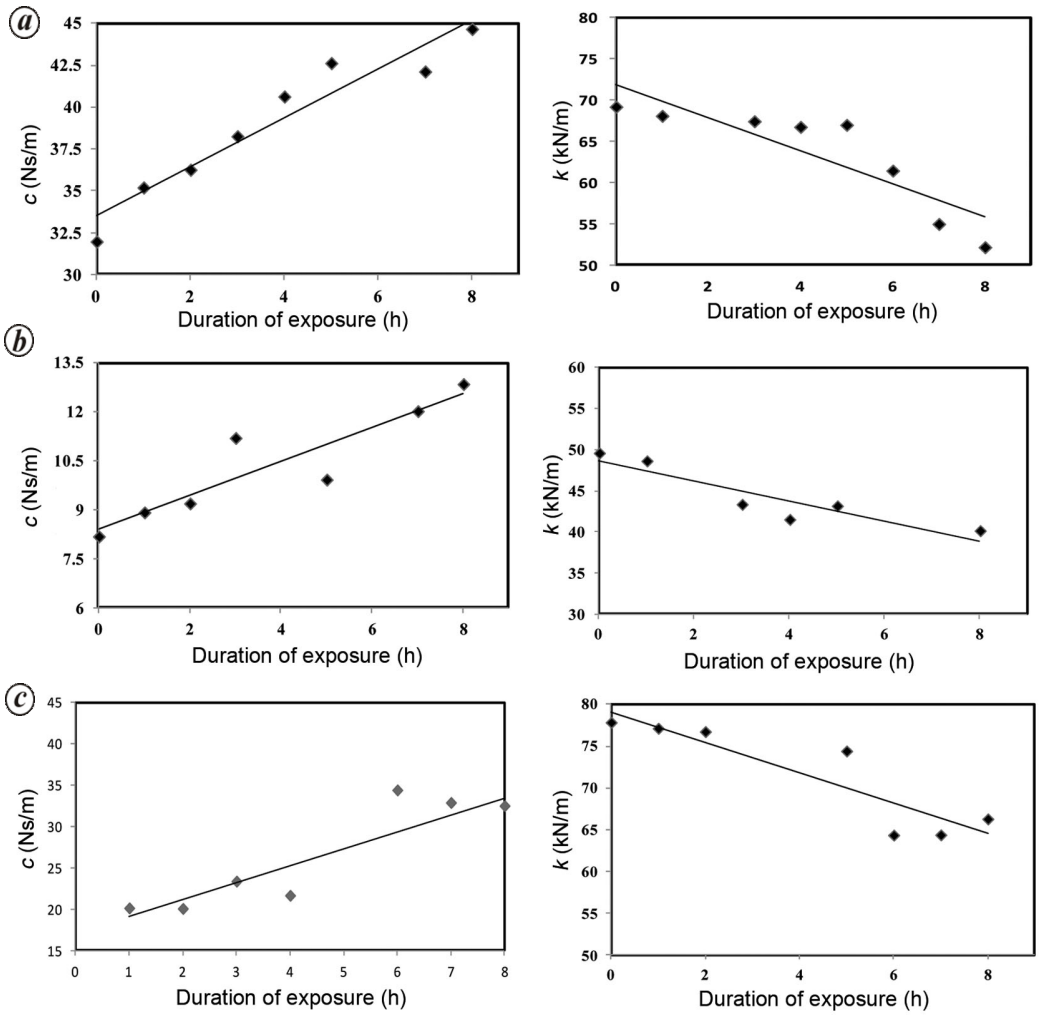

Figure 9. Variation of extracted system parameters (stiffness and damping): ***a***, Specimen 1; ***b***, Specimen 2; ***c***, Specimen 3.

impedance $Z_{s,\text{eff}}$ consists of the real and imaginary components x and y respectively. A close examination of the extracted impedance components in the frequency range 100–110 kHz of the healthy state revealed that the system behaviour was similar to that of a Kelvin–Voigt system, i.e. a parallel arrangement of a spring element (k) with a damper (c), shown in Figure 7 *a*, for which the real and imaginary components are given by Hixon[41] as

$$x = c \text{ and } y = -\frac{k}{\omega}. \tag{10}$$

Within the frequency range 100–110 kHz, x was found to possess more or less a constant positive value and y a negative value with magnitude decreasing with frequency, similar to the characteristic of the Kelvin–Voigt system as shown in Figure 7 *b–d* for all the three specimens. For the Kelvin–Voigt system, the value of stiffness (k) is basically equal to the slope of plot of y with ω^{-1} (eq. (10)), which should be a straight line. This is confirmed in Figure 8 *a–c*, which show the plot of y versus ω^{-1} for specimens 1–3 corresponding to different levels of corrosion. For all the three specimens, with the advancement of corrosion, the slope of the curve decreases consistently. Using eq. (10), the values of k and c were determined for all specimens after each hour of exposure to accelerated corrosion. Figure 9 *a–c* displays the effect of corrosion severity (in terms of the number of hours of application of constant current) on the identified equivalent structural parameters (c and k). With the progression of corrosion the damping can be observed to increase by about 41%, 38% and 30% and the identified stiffness reduce by 19%, 16% and 29% for specimens 1, 2 and 3 respectively, for an exposure time of 8 h of accelerated corrosion.

Using the Kelvin–Voigt system and equivalent stiffness obtained from that system, Bhalla *et al.*[40] realistically quantified fatigue-induced damage in bolted double-lap joints to predict the remaining useful life of the component by surface-bonded PZT patches. They found that the approach based on the equivalent k is an improvement over statistical indicators, such as root mean square deviation (RMSD) of raw conductance, which fail to provide meaningful quantification of the loss of stiffness of the component.

Previously, Soh and Bhalla[42] had used the same Kelvin–Voigt system for the nondestructive evaluation of concrete, covering both strength prediction and damage assessment. The identified equivalent parameters extracted from the impedance sprectrum were found to be sensitive to structural damages as well as to concrete strength gain during curing. They found this technique much superior to the existing strength prediction techniques such as the ultrasonic pulse velocity methods. The new method demands only one free surface of the specimen against two opposite surfaces in the ultrasonic methods.

Although the Kelvin–Voigt system-based analysis showed consistent results, the identified system (parallel spring–damper combination) does not include mass element, which is expected to play a significant role due to loss of mass associated with the corrosion process. So, a close observation of frequency range 250–300 kHz showed that the system behaviour was similar to a series combination of spring, damper and mass, such as the one shown in Figure 10 *a*. For this combination, the system parameters are related to x and y as[41]

$$x = \frac{c^{-1}}{c^{-2} + \left(\frac{\omega}{k} - \frac{1}{\omega m}\right)^2} \text{ and } y = \frac{-\left(\frac{\omega}{k} - \frac{1}{\omega m}\right)^2}{c^{-2} + \left(\frac{\omega}{k} - \frac{1}{\omega m}\right)^2}. \tag{11}$$

The angular frequency at which $y = 0$ is denoted by ω_0. Using eq. (11), the system parameters can be determined by algebraic manipulations as

$$m = \frac{k}{\omega_0^2}, \tag{12}$$

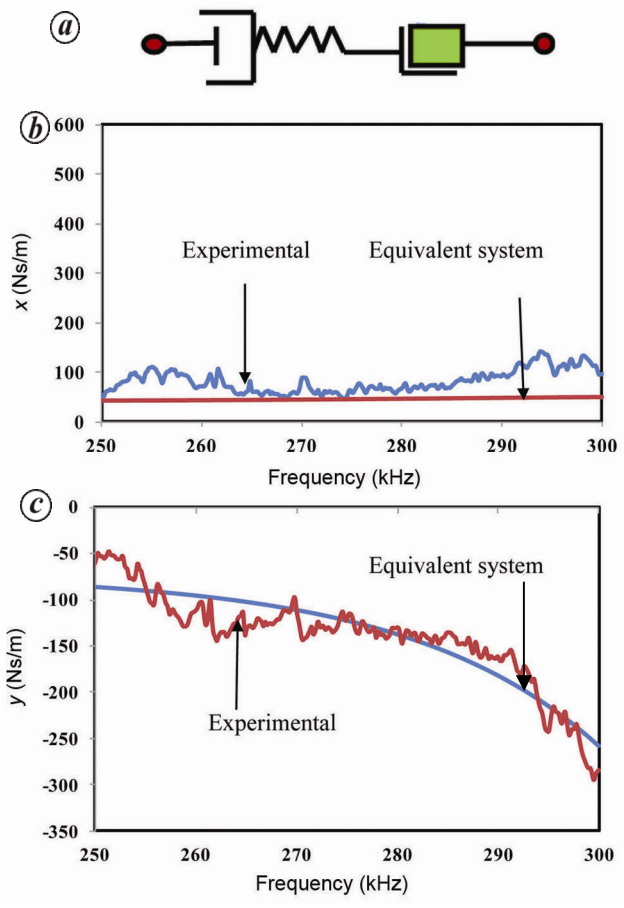

Figure 10. Equivalent system parameters. ***a***, Equivalent system (series combination of spring-damper and mass); ***b***, x versus f of specimen 1; ***c***, y versus f of specimen 1.

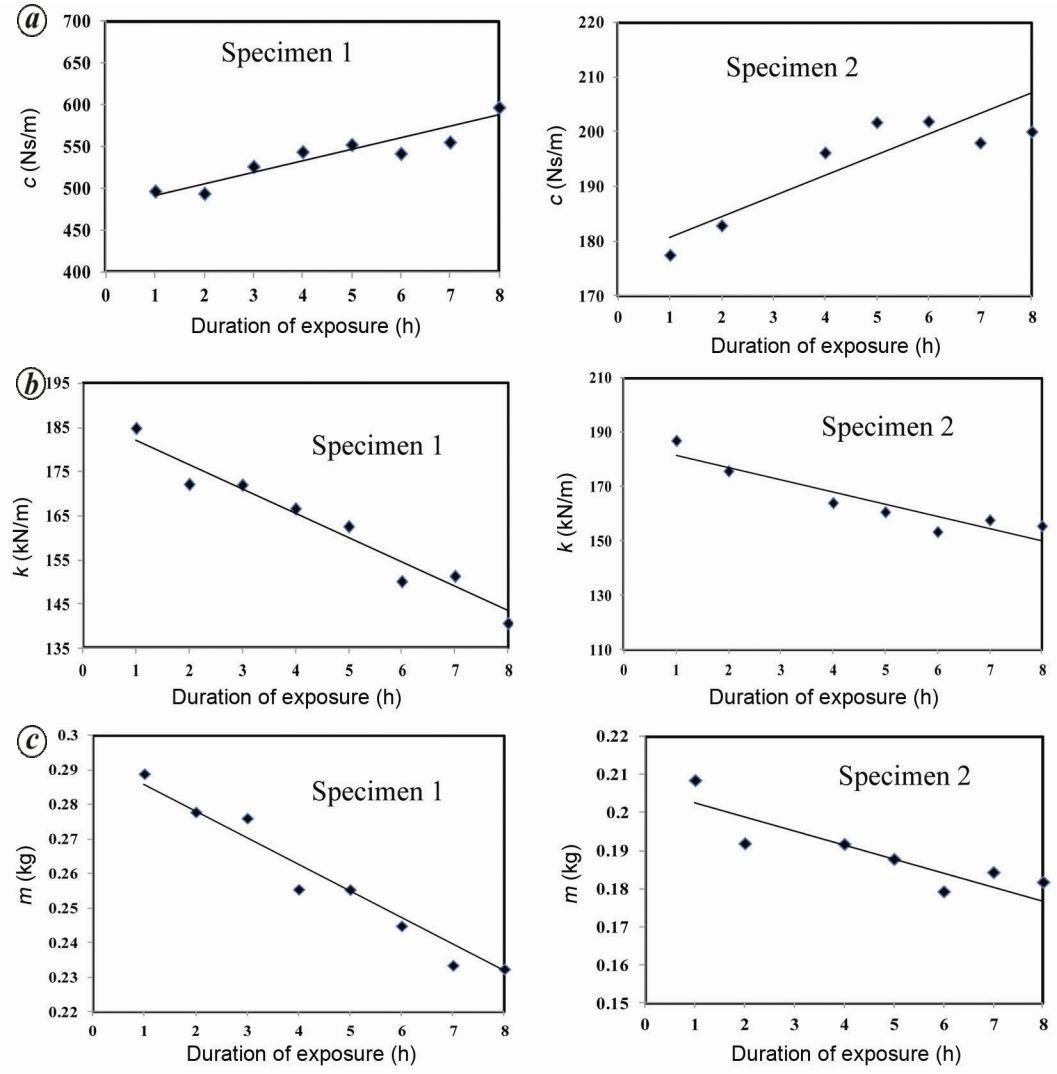

Figure 11. Variation of extracted system parameters: ***a***, Equivalent damping of specimens 1 and 2; ***b***, Equivalent stiffness of specimens 1 and 2; ***c***, Equivalent mass of specimens 1 and 2.

$$k = -\frac{x^2 + y^2(\omega^2 - \omega_0^0)}{\omega y}, \tag{13}$$

and

$$c = \frac{x^2 + y^2}{x}. \tag{14}$$

The analytical plots of x and y obtained by equivalent parameters match well with their experimental counterparts for specimen 1, as shown in Figure 10 *b* and *c*. Specimen 2 also followed a similar trend in the frequency range 250–300 kHz. However, specimen 3 was an exception and was therefore not considered for analysis using this model. The system parameters, i.e. equivalent spring constant, equivalent mass and equivalent damping constant were determined for specimens 1 and 2 using the eqs (12)–(14) after each hour of corrosion exposure. The identified equivalent damping increased by 25% and 23%, equivalent stiffness was found to reduce by 27% and 20% and the equivalent mass reduced by 20% and 25% for specimens 1 and 2 respectively, after 8 h of exposure. The variation of the system parameters with increasing corrosion exposure for this system is shown in Figure 11. For this model, the relative reduction in the equivalent mass is agreeable between the two specimens.

During the experiment, the actual mass of the specimen was also measured to correlate with the PZT-identified equivalent mass. Figure 12 shows a plot of the relative mass loss for the specimens (measured directly by removing the specimens from the accelerated corrosion exposure after each hour) with the progression of corrosion. For the purpose of quantification, mass loss can be expressed in non-dimensional form as

$$\Delta m = \delta m / m_0, \tag{15}$$

where m_0 is the original mass of the specimen and δm is the loss of mass. Here both the actual and the

PZT-identified mass (using eq. (12)) can be substituted. This index defines the severity of corrosion in the present scenario.

Although the values of m so determined by the PZT patches differed from the actual mass of the specimen (comparing Figures 11 *c* and 12), the loss of the PZT-identified $\delta m/m_0$ reasonably correlates with the loss of the actual $\delta m/m_0$ of the specimens, as shown in Figure 13. Hence, the PZT identified mass can provide a reasonable estimation of the actual mass loss of the specimen. For the purpose of correlating both, the two are related by a non-dimensional mass model as:

$$(\delta m/m)_{\text{actual}} = \lambda(\delta m/m)_{\text{PZT}}, \tag{16}$$

Based on the data averaged over the two patches spanning over the two specimens, the value of λ is found to be 4.974. This model can be directly used, with no requirement of determining the absolute mass of the specimen as it gives the loss of mass directly.

Comparison of the proposed method with conventional methods

Several damage metrics can be used to mathematically quantify the damage while reducing the admittance data to a single scalar value. The root mean square deviation (RMSD) metric was used because it is an established statistical metric to quantify damage[43,44]. The RMSD metric is defined as:

$$\text{RMSD} = \sqrt{\frac{\sum_{1}^{N}(G_i - G_i^0)^2}{\sum_{1}^{N}(G_i^0)^2}} \times 100, \tag{17}$$

where G_i is the conductance of the PZT patch at any stage during the test and G_i^0 is the baseline value (in pristine condition), i representing the frequency index (100–300 kHz). Figure 14 shows the variation of RMSD indices of the three specimens as a function of the duration of accelerated corrosion exposure. For specimen 1, the RMSD index appears to follow a crudely linear trend (Figure 14 *a*). For specimen 2, it increases abruptly after the first hour and then exhibits a weakly linearly increasing trend (Figure 14 *b*). However, for specimen 3 (Figure 14 *c*), essentially a scatter of values can be observed. Although all the three bars are identically affected, since the specimen as well as the exposure conditions are identical, the overall magnitude of the RMSD index differs significantly from specimen to specimen. Hence, it has not able to provide damage-related information regarding the corrosion severity consistently. This is not unexpected, since RMSD is a statistical quantifier[40].

Compared to the variation of the RMSD index, the observed variations in indentified equivalent parameters obtained from the Kelvin–Voigt system and series combination of spring, damper and mass system are much more agreeable (Figures 9 and 11).

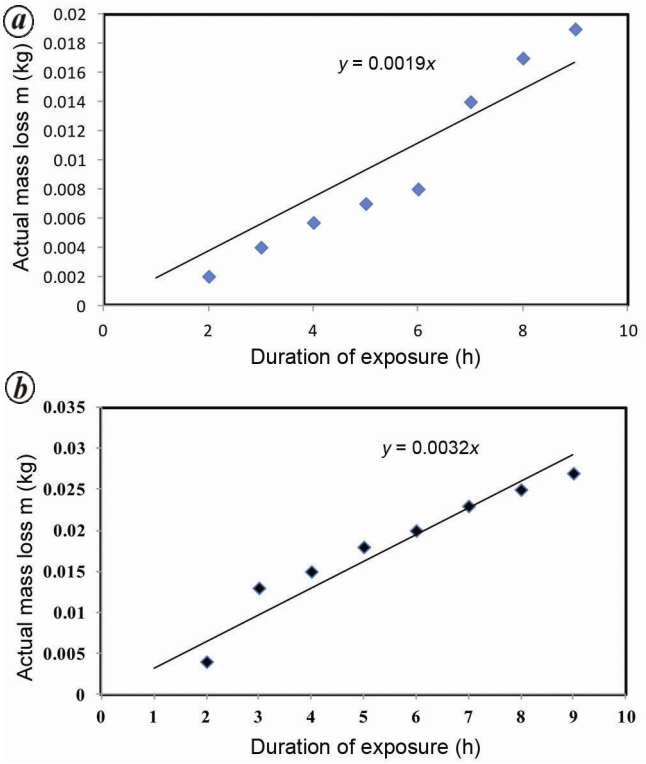

Figure 12. Variation of actual mass loss with accelerated corrosion exposure. ***a***, Specimen 1; ***b***, Specimen 2.

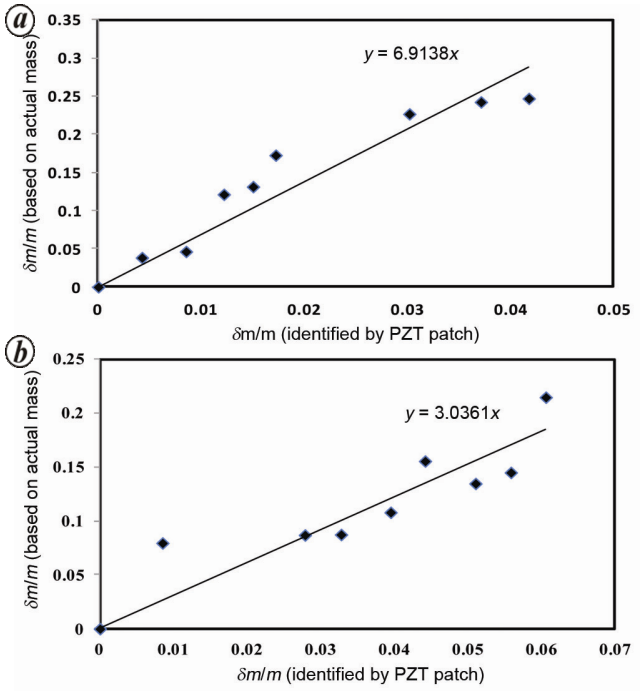

Figure 13. Correlation between loss of actual mass with PZT-identified mass loss. ***a***, Specimen 1; ***b***, Specimen 2.

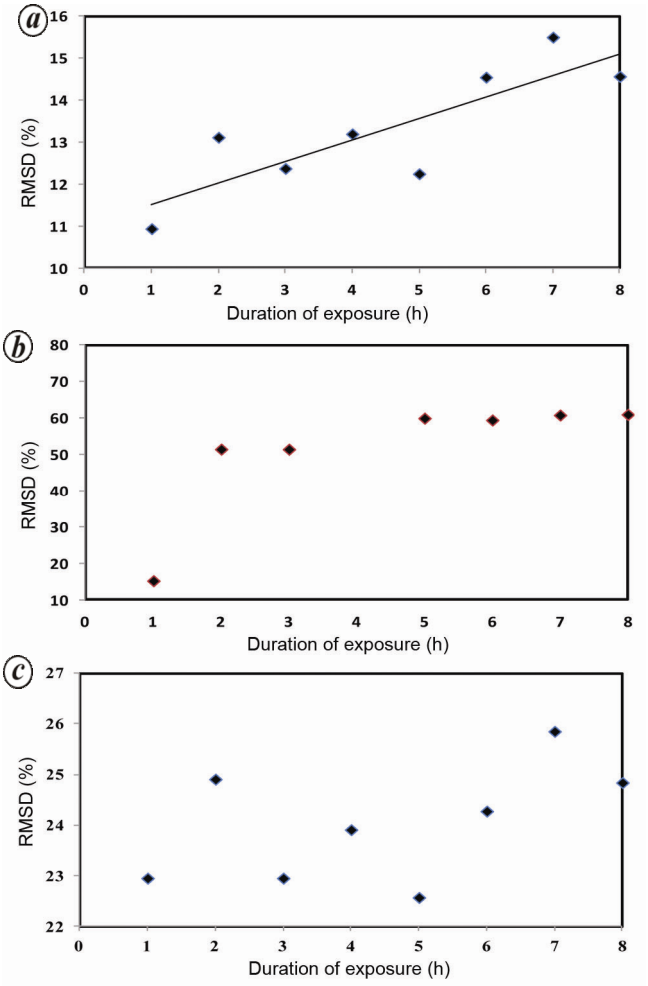

Figure 14. Variation of RMSD: ***a***, Specimen 1; ***b***, Specimen 2; ***c***, Specimen 3.

The experimental results were also verified using conventional half-cell potential (using ACM field machine). When the PZT-identified mass loss obtained from series combination of spring, damper and mass system changed from 0.15 to 0.21 kg, the half-cell potential reading changed from –394 to –501 mv for specimen 1, which can be interpreted as high probability of corrosion according to ASTM standards[45]. A simple comparison of these potential data with the ASTM guidelines on rebar corrosion probability has been criticized by several researchers, as a more negative reading of potential, which is generally considered to indicate a higher probability of corrosion, may not always be valid as many factors can shift the potential readings towards more positive or negative values[46,47].

This model-based approach derived is more reliable compared to the conventional half-cell potential values because the value of the half cell potential difference will depend on various factors such as type of electrode used, concrete porosity, etc. Further, the half-cell potential measurements do not provide quantitative information on the actual corrosion rate of rebars. They need to be interpreted in the context of complementary data from the concrete structures by specialists or skilled engineers. The approach presented here, however, is more practical, direct and consistent.

Conclusion

This article has extended the application of a potentially new corrosion assessment approach based on the EMI technique which employs surface-bonded PZT patches utilizing the extracted structural parameters from the impedance spectrum. Better response of the equivalent extracted parameters k and m, is observed compared to the RMSD index, as it makes use of real as well as imaginary components of admittance signature for extracting damage-sensitive equivalent structural parameters. This model-based approach using equivalent structural parameters is an improvement over the statistical indicators, such as RMSD, which fail to provide meaningful indication of the loss of stiffness and mass of the specimens. Further, the identified mass from the observed model (series combination of spring–damper and mass) follows a consistent behaviour with the progress of corrosion and the relative loss of the identified mass correlates well with the relative loss of actual mass of the specimens. The half-cell potential measurements obtained also strongly indicate the occurrence of corrosion. However, the EMI technique provides more information. For new constructions of significance, this approach can be utilized for prior assessment of corrosion in reinforcement bars before embedding them in concrete, as they are vulnerable to get corroded when exposed to chloride-laden environment.

1. Montemor, M. F. and Simoes, A. M. P., Chloride induced corrosion on reinforcing steel: from the fundamentals to the monitoring technique. *Cem. Concr. Compos.*, 2003, **25**, 491–502.
2. Li, C. Q., Life-cycle modelling of corrosion-affected concrete structures: propagation. *J. Struct. Eng., ASCE*, 2003, **129**, 753–761.
3. Li, C. Q., Time dependent reliability analysis of the serviceability of corrosion affected concrete structures. *J. Mater. Struct.*, 2005, **3**, 105–116.
4. Li, C. Q., Zheng, J. J., Lawanwisut, W. and Melchers, R. E., Concrete delamination caused by steel reinforcement corrosion. *J. Mater. Civil Eng., ASCE*, 2007, **19**, 591–600.
5. Liang, C., Sun, F. P. and Rogers, C. A., Coupled electromechanical analysis of adaptive material systems – determination of the actuator power consumption and system energy transfer. *J. Intell. Mater. Syst. Struct.*, 1994, **5**, 12–20.
6. Giurgiutiu, V. and Rogers, C. A., Electromechanical impedance method for structural health monitoring and non-destructive evaluation. In Proceeding of International Workshop on Structural Health Monitoring, Stanford, California, 1997, pp. 802–812.
7. Giurgiutiu, V. and Zagrai, A., Characterization of piezoelectric wafer active sensors. *J. Intell. Mater. Syst. Struct.*, 2000, **11**, 959–76.
8. Giurgiutiu, V., Damage metric algorithms for active-sensor, structural health monitoring, In First European Workshop on Structural Health Monitoring, Paris, France, 2002, pp. 433–441.

9. Park, G., Cudney, H. H. and Inman, D. J., Impedance-based health monitoring of civil structure components. *J. Infrastruct. Syst., ASCE*, 2000, **6**(4), 153–160.
10. Park, G., Cudney, H. H. and Inman, D. J., An integrated health monitoring technique using structural impedance sensors. *J. Intell. Mater. Syst. Struct.*, 2000, **11**, 448–455.
11. Bhalla, S. and Soh, C. K., Structural impedance based damage diagnosis by Piezo-transducers. *Earthquake Eng. Struct. Dyn.*, 2003, **32**, 1897–1916.
12. Bhalla, S. and Soh, C. K., High frequency piezoelectric signatures for diagnosis of seismic/blast induced structural damages. *NDT&E Int.*, 2004, **37**, 23–33.
13. Shanker, R., Bhalla, S. and Gupta, A., Dual use of PZT patches as sensors in global dynamic and local EMI techniques for structural health monitoring. *J. Intel. Mater. Syst. Struct.*, 2011, **22**, 1841–1856.
14. Bhalla, S., Soh, C. K. and Liu, Z., Wave propagation approach for NDE using surface bonded piezoceramics. *NDT&E Inter.*, 2005, **38**, 143–150.
15. Bhalla, S., Naidu, A. S. K. and Soh, C. K., Influence of structure–actuator interactions and temperature on piezoelectric mechatronic signatures for NDE. Proceedings in SPIE Conference on Smart Materials, Structures, and Systems, Bengaluru, 12–14 December 2003, vol. 5062, pp. 263–269.
16. Park, S., Yun, C. B., Roh, Y. and Lee, J. J., Health monitoring of steel structures using impedance of thickness modes at PZT patches. *Smart Struct. Syst.*, 2005, **1**(4), 339–353.
17. Park, S., Yun, C. B., Roh, Y. and Lee, J. J., PZT-based active damage detection techniques for steel bridge components. *Smart Struct. Syst.*, 2006, **15**(4), 957–966.
18. Park, G., Farrar, C. R., Rutherford, C. A. and Robertson, A. N., Piezoelectric active sensor self-diagnostics using electrical admittance measurements. *J. Vib. Acoust., ASME*, 2006, **128**(4), 469–476.
19. Visalakshi, T. and Bhalla, S., Review of impedance based structural health monitoring. Proceedings of the International Conference, VETOMAC VI, IIT Delhi, December 2010, pp. 550–557.
20. Bhalla, S. and Soh, C. K., Structural health monitoring by Piezo-impedance transducer: application. *J. Aerosp. Eng., ASCE*, 2004, **17**, 166–171.
21. Rothwell, G. P., Corrosion monitoring: some techniques and applications. *NDT&E Int.*, 1978, **11**, 108–111.
22. Pradhan, B., Performance of TMT and CTD steel bars, OPC and blended cements against chloride induced rebar corrosion in concrete, Ph D thesis, IIT Delhi, 2007.
23. Andrade, C., Alonso, C. and Sarria, J., Corrosion rate evolution in concrete structures exposed to the atmosphere. *Cem. Concr. Compos.*, 2002, **24**, 55–64.
24. Hussain, S. E., Rasheeduzzafar, A., Musallam, A.-A. and Gahtani, A. S-.A. Factors affecting threshold chloride for reinforcement corrosion in concrete. *Cement Concrete Res.*, 1995, **25**, 1543–1555.
25. Fuhr, P. L. and Huston, D. R., Corrosion detection in reinforced concrete roadways and bridges via embedded fiber optic sensor. *Smart Mater. Struct.*, 1998, **7**, 217–228.
26. Grattan, S. K. T., Basheer, P. A. M., Taylor, S. E., Zhao, W., Sun, T. and Grattan, K. T. V., Fiber Bragg grating sensors for reinforcement corrosion monitoring in civil engineering structures. *Am. J. Phys.*, 2007, **76**, 12–18.
27. Grattan, S. K. T., Basheer, P. A. M., Taylor, S. E., Zhao, W., Sun, T. and Grattan, K. T. V., Monitoring of corrosion in structural reinforcing bars: performance comparison using *in situ* fiber–optic and electric wire strain gauge systems. *IEEE Sensors J.*, 2009, **9**, 1484–1502.
28. Zheng, Z. P., Sun, X. N. and Lei, Y., Monitoring corrosion of reinforcement in concrete structures via fibre grating sensors. *Front. Mech. Eng. China*, 2009, **4**, 316–319.
29. Zheng, Z., Lie, Y. and Sun, Z., Measuring corrosion of steels in concrete via fiber Bragg grating sensors – Lab experimental test and in-field application. Earth and Space 2010; Engineering, Science, Construction, and Operations in Challenging Environments, ASCE, 2010.
30. Gao, J., Wu, J., Li, J. and Zhao, X., Monitoring of corrosion in reinforced concrete structure using Bragg grating sensing. *NDT&E Int.*, 2011, **44**, 202–205.
31. Park, S. and Park, S. K., Quantitative corrosion monitoring using wireless electromechanical impedance measurements. *Res. Nondestruct. Eval.*, 2010, **21**, 184–192.
32. Park, S., Benjamin, L. G., Inman, J. and Yun, C. B., MFC-based structural health monitoring using a miniaturized impedance measuring chip for corrosion detection. *Res. Nondestruct. Eval.*, 2007, **18**, 139–150.
33. Simmers, G. E., Impedance-based structural health monitoring to detect corrosion, MS thesis, Blacksburg, Virginia, 2005.
34. Rathod, V. T. and Mahapatra, D. R., Ultrasonic lamb wave based monitoring of corrosion type of damage in plate using a circular array of piezoelectric transducers. *NDT&E Int.*, 2011, **44**, 628–636.
35. Talakokula, V., Bhalla, S. and Gupta, A., Corrosion assessment of reinforced concrete structures based on equivalent parameters using electro-mechanical impedance technique. *J. Intel. Mater. Syst. Struct.*, 2014, **25**(4), 484–500.
36. Talakokula, V. and Bhalla, S., Reinforcement corrosion assessment capability of surface bonded and embedded piezo sensors for RC structures. *J. Intell. Mater. Syst. Struct.*, 2014; doi:10.1177/1045389X14554133.
37. PI Ceramics, Product information catalogue, Lindenstrabe, Germany, 2012, www.piceramic.de
38. Agilent Technologies, Test and measurement catalogue, USA, 2012.
39. Scientech Technology, 2011; http://www.scientech.bz (accessed on 20 August).
40. Bhalla, S., Vittal, A. P. R. and Veljkovic, M., Piezo-impedance transducers for residual fatigue life assessment of bolted steel joints. *J. Struct. Health Monit.*, 2012, **11**(6), 733–750.
41. Hixon, E. L., *Mechanical Impedance, Shock and Vibration Handbook* (ed. Harris, C. M.), McGraw Hill, New York, 1988, pp. 10.1-10.46.
42. Soh, C. K. and Bhalla, S., Calibration of piezo-impedance transducers for strength prediction and damage assessment of concrete. *Smart Mater. Struct.*, 2005, **14**(4), 671–684.
43. Giurgiutiu, V. and Rogers, C. A., Recent advancements in the rlectro-mechanical (E/M) impedance method for structural health monitoring and NDE. In Proceedings of SPIE Conference on Smart Structures and Integrated Systems, San Diego, California, March, 1998, vol. 3329, pp. 536–547.
44. Giurgiutiu, V., Reynolds, A. and Rogers, C. A., Experimental investigation of E/M impedance health monitoring for spot-welded structural joints. *J. Intel. Mater. Syst. Struct.*, 1999, **10**, 802–812.
45. ASTM C876-91, Standard test method for half-cell potentials of uncoated reinforcing steel in concrete, West Conshohocken, PA, 1999.
46. Gu, G. P., Carter, P., Beaudoin, J. J. and Arnott, M., Validation of half-cell potential data from bridge decks. *Constr. Repair*, 1996, **10**(3), 18–20.
47. Elsener, B., Andrade, C., Gulikers, J., Polder, R. and Raupach, M., Half-cell potential measurements-potential mapping on reinforced concrete structures. (RILEM TC 154-EMC recommendation). *Mater. Struct.*, 2003, **36**, 461–471.

Received 8 December 2014; revised accepted 3 March 2015